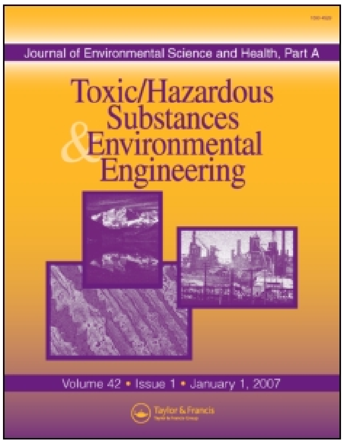

Journal of Environmental Science and Health, Part A
Publication details, including instructions for authors and subscription information:
http://www.informaworld.com/smpp/title~content=t713597268

REMOVAL DYNAMICS OF AIRBORNE ROAD DUST IN A VENTILATED AIRSPACE

Chung-Min Liao [a]; Mei-Yu Huang [a]; Jein-Wen Chen [a]; Tsang-Jung Chang [a]
[a] Department of Bioenvironmental Systems Engineering, National Taiwan University, Taipei, Taiwan, ROC

Online Publication Date: 12 June 2002

To cite this Article Liao, Chung-Min, Huang, Mei-Yu, Chen, Jein-Wen and Chang, Tsang-Jung(2002)'REMOVAL DYNAMICS OF AIRBORNE ROAD DUST IN A VENTILATED AIRSPACE',Journal of Environmental Science and Health, Part A,37:6,1009 — 1027

To link to this Article: DOI: 10.1081/ESE-120004519

URL: http://dx.doi.org/10.1081/ESE-120004519

J. ENVIRON. SCI. HEALTH, A37(6), 1009–1027 (2002)

REMOVAL DYNAMICS OF AIRBORNE ROAD DUST IN A VENTILATED AIRSPACE

Chung-Min Liao,* Mei-Yu Huang, Jein-Wen Chen, and Tsang-Jung Chang

Department of Bioenvironmental Systems Engineering, National Taiwan University, Taipei, Taiwan 10617, ROC

ABSTRACT

We derive a simple linear dynamic equation to describe the removal mechanisms of airborne road dust from a ventilated airspace. The dynamic equation is sufficiently to take into account the simultaneous removal effects of turbulent coagulation, turbulent diffusive deposition, gravitational sedimentation, and airflow pattern within a ventilated airspace. Three dimensionless parameters TC, TD, and GS that characterize the relative effects of turbulent coagulation, turbulent diffusive deposition and gravitational settling, respectively, in a ventilated airspace were introduced to generalize the removal dynamics of airborne road dust. An environmental chamber test was carried out not only to determine the particle size distributions but also to verify the removal dynamics of airborne road dust in a ventilated airspace. Our results demonstrate that there is no significant variation for particle size distributions of road dust obtained from urban and suburban areas in north Taiwan region and both followed a lognormal distribution with average geometric mean diameter of $1.08 \pm 0.02\,\mu m$ and geometric standard deviation of 2.59 ± 0.03. Measured values match the simulated values with an r^2 value of 0.93, whereas the overall RMSE value of $2.36 \pm 1.05\,mg\,m^{-3}$ is low, indicating that the ability to predict the removal dynamics of airborne road dust within a ventilated airspace using an average particle size based linear equation.

*Corresponding author. E-mail: cmliao@ccms.ntu.edu.tw

Effects of TC, TD, GS, and various ventilation systems on the time-dependent road dust concentrations are also justified.

Key Words: Road dust; Ventilation; Particle size distribution; Coagulation; Deposition

INTRODUCTION

Paved road dust attributable to the indoor air in urban residence houses has been the most serious indoor air pollution in Taiwan region.[1–3] Paved road dust present on the surface of streets may consist of a complex mixture of soil dust, deposited motor vehicle exhaust particles, tire dust, brake lining wear dust, plant fragments, and other biological materials. Pope and Dockery,[4] Dockery et al.,[5] Schwartz,[6] Seaton et al.,[7] and Ackermann-Liebrich et al.[8] in their epidemiological studies indicated that the particulate matter in outdoor road dust air was strongly associated with lung function parameters, respiratory symptoms and mortality. These findings were especially pronounced for inhaled thoracic particles (particles of aerodynamic equivalent diameter (AED) less than 10 μm, PM_{10}) and fine particles (particles smaller than 2.5 μm AED, $PM_{2.5}$).

Miguel et al.[9] reported that paved road dust when entrained into the atmosphere by passing traffic is a source of allergen exposure for the general population in that 5–12% of the allergenicity of atmospheric total suspended particulate matter samples is attributable to paved road dust emission. Tiittanen et al.[10] suggested that there was a high correlation between resuspended road dust and respiratory health among symptomatic children. Hirsch et al.[11] indicated that exposure to road dust may associate with the allergic sensitization, whereas concentrations of aerial road dust were sufficient to create an unhealthy work environment.

Reducing indoor airborne particulate to acceptable levels can be carried out in a number of ways. A dust collection device may be considered that can range from a cyclone to a dry particulate filter. When considering type of filter media, size of the unit and energy consumption, the operating costs of dust removal are high. Many factors will affect the emission factor of the road dust in the field, including water content of the road dust, wind speed, mechanical disturbance, silt loading and so on.[12–14] As most time of 70–90% is spend indoors, information on the indoor and outdoor relationship of road dust concentrations is important. In the indoor environment, the removal of entrained airborne road dust occurs through ventilation and deposition. The types of ventilation, the outdoor levels, and climate can influence indoor particles concentration of airborne road dust. Therefore, a study of the airborne road dust removal from a ventilated airspace is of fundamental and practical significance.

In a ventilated airspace, the time-dependent change in dust properties, such as particle size distribution and particle number and mass concentrations, are determined by considering the simultaneous effects of coagulation, diffusion, deposition, sources, distribution of supplied air, etc., occurring with the enclosure. Coagulation, for example, increases the size of dust particles, resulting in a decrease in concentration. Diffusion decreases the concentration of dust particles as a result of the deposition of small particles on wall surfaces, whereas gravitational settling decreases the concentration results from deposition of larger particles on the floor.

Friedlander,[15] Okuyama et al.,[16] Rogge et al.,[17] Kleeman and Cass,[18] Wang et al.,[19] Liao and Singh,[20] Liao et al.[21] and among others have been presented the theoretical and experimental studies on this mode of removal. Friedlander[15] pointed out that the general dynamic equation associated with the Navier-Stokes equation can be used to represent dust and airflow distribution, it is extremely difficult, if not impossible, to solve exactly. Experimental studies, on the other hand, have been carried out by observing the change in mass concentration and particle size distribution of aerosol in an observation chamber. The results, however, are obtained under specific conditions and appear insufficient to predict the general behavior under various ventilation systems. The problem becomes more difficult for ventilation systems with multiple inlets and outlets. Road dust behavior in a ventilated airspace, however, has not been established satisfactorily for urban residence houses in Taiwan region.

The purpose of this study is to develop a simple modeling approach towards the removal dynamics of airborne road dust concentration undergoing turbulent coagulation, turbulent diffusive deposition, gravitational settling, and ventilation airflow in a ventilated airspace. The verification of the model in predicting the distributions of airborne road dust concentration was presented by using a chamber test under various ventilation modes, ventilation rates and road dust generation rates. The particle size distributions of road dust obtained from urban and suburban areas were also determined.

MATERIALS AND METHODS

Environmental Chamber Experiment

The test facilities used in the experimental studies were comprised of an environmental chamber, an air delivery system, a road dust generation system, and a road dust sampling and analyzing system. All components were housed within a laboratory maintained at a temperature of $27 \pm 0.5^{\circ}$C and a relative humidity ranged from 60 to 70%.

Experiments were carried out in a test chamber measuring $90 \times 90 \times 90$ cm. Figure 1 gives the dimensions and general outline of the test chamber.

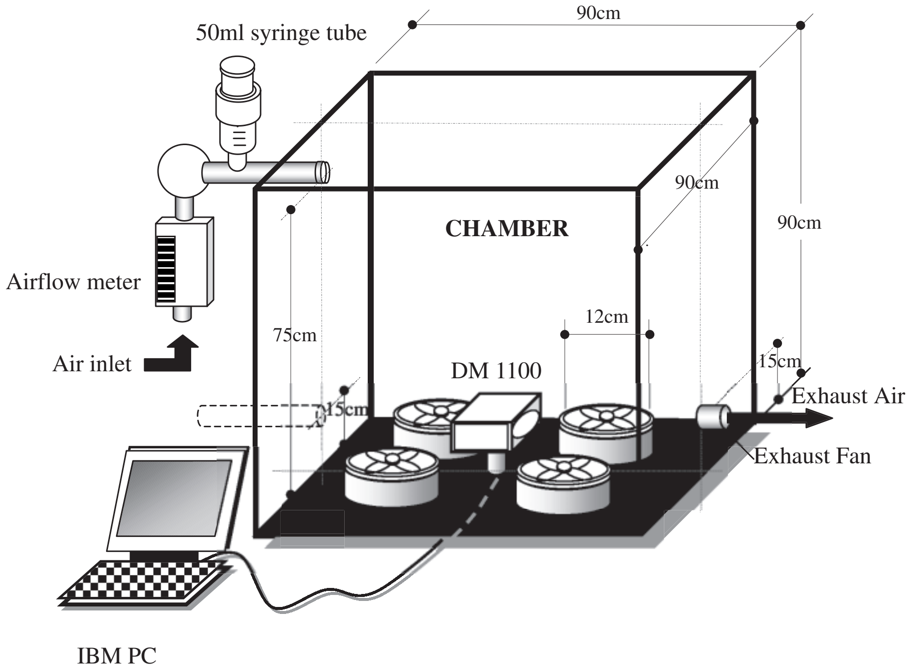

Figure 1. Schematic diagram showing the overall view of environmental chamber and experimental equipment.

The dimensions were such as to simulate one slot-ventilated enclosure with an negative pressure ventilation system. The chamber, fabricated from Plexiglas, had 4 small 12 cm fans located on the floor of the chamber for maintaining uniform mixing of the road dust particles throughout the chamber.

Air entered the chamber through a circular slot inlet with diameter of 5 cm. The exhaust location was 15 cm from floor level measured to the center of the outlet. The chamber was mechanically ventilated by means of an air pump delivering two ventilation rates, 140 ± 13 and $280 \pm 15\,cm^3\,s^{-1}$, which were determined by an airflow meter (S-110-3 Flow Meter, McMillan Inc., USA) with an output in $cm^3\,s^{-1}$. Two inlet locations of 15 and 75 cm above the floor, respectively, were employed to simulate the displacement and shirt-circuit ventilation systems (Fig. 1).

Two kinds of road dust particle that collected from urban and suburban areas located at north Taiwan region were used in this experiment. Experimental Road dust was stored in a 50 mL syringe tube. The syringe plunger was depressed a constant distance once a minute and the contents were introduced into the chamber via the supplied airflow. Two road dust source generation rates measured to be 0.25 and $0.5\,g\,mim^{-1}$, respectively, were used in the chamber test.

A portable laser dust monitor (Series 1100, Grimm Labortechnik GmbH & Co. KG, Ainring, Germany; referred to as DM1100) was used to analyze the airborne dust characteristics. The DM1100 combines the principles of aerodynamic particle size separation and light scattering particle detection. The particles can range from 0.5 to 10 μm AED. The DM1100 measured dust mass concentrations in the range of 1.0 to 50 000 $\mu g\, m^{-3}$. Measured channels are in the ranges of 0.5–1, 1–2, 2–5, 5–10, and >10 μm AED. Before the measurements, the DM1100 was calibrated with known particles of Uniform Latex Microspheres Polystyrene (0.5 μm) and Polymer Microspheres Styrene Vinyltoluene (3 μm) (Duke Scientific, Palo Alto, CA). The DM1100 was operated at the design sampling flow rate of $1.2\, L\, min^{-1} \pm 10\%$. The outputs from DM1100 can be expressed both as $\mu g\, m^{-3}$ and as particles L^{-1}. A portable IBM PC was used to collect all sampling data.

Experimental road dust particles were sampled every 1 min to determine the rate of change in concentration in that DM1100 needs 5 s to record each reading. It took 0.5 h to measure the concentration changes in each experiment. The chamber was cleaned before and after each experiment.

Mathematical Model

A ventilated airspace where the system boundary is taken as the walls, floor, and ceiling of the enclosure is shown in Figure 2 in that a time-dependent road dust source is introduced from the outdoor and

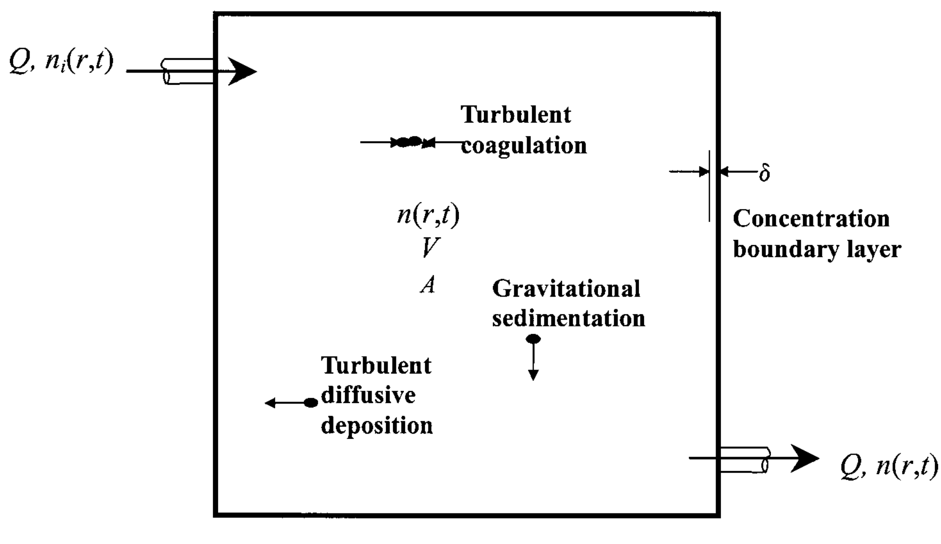

Figure 2. Schematic diagram showing the removal mechanisms of airborne road dust in a ventilated airspace.

entrained into the ventilated airspace with volume $V(\mathrm{m}^3)$ and a wall surface area $A(\mathrm{m}^2)$.

Before deriving the dynamic equation to describe the road dust concentration change within a ventilated airspace, the following assumptions are made to simplify the physical properties: (i) the road dust introduced from outdoor into the ventilated airspace is instantaneously dispersed uniformly throughout the enclosure, (ii) no gas-to-particle conversion occurs within the system, (iii) no external forces act on the particle other than gravity, (iv) particles have an AED and are electrically neutral, (v) particles collide with each other to form a single new spherical particle whose mass is the same as the combined mass of the two smaller particles, and (vi) the road dust particle concentration is spatially uniform in the system volume except across the boundary layer where the concentration changes linearly within the layer.

Friedlander,[15] Liao et al.,[21] Greenfield et al.,[22] Okuyama and Kousaka,[23] Liao et al.[24] and among others have been used the population-balance model to describe the time-dependent change in properties of an airborne dust undergoing turbulent coagulation, turbulent diffusive deposition, gravitational settling, and ventilation airflow. By using the population-balance model, the road dust dynamics in a ventilated airspace can be expressed as (Fig. 2),

$$\begin{aligned}\frac{\partial n(r,t)}{\partial t} = \frac{1}{2}\int_{\rho=0}^{\rho=r/2^{1/3}} & K\Big(\big(r^3-\rho^3\big)^{1/3},\rho\Big)n\Big(\big(r^3-\rho^3\big)^{1/3},t\Big)n(\rho,t) \\ & \times\left(\frac{r}{(r^3-\rho^3)^{1/3}}\right)^2 d\rho - \int_0^\infty K(r,\rho)n(r,t)n(\rho,t)\,d\rho - (D(r)+\varepsilon) \\ & \times\frac{S}{\delta V}n(r,t) - \frac{U_s(r)}{H}n(r,t) - \frac{Q}{V}n(r,t) + \frac{G(r,t)}{V}, \qquad (1)\end{aligned}$$

where $n(r,t)$ is the particle concentration of road dust of radius r (particles $\mathrm{cm}^{-3}\mu\mathrm{m}^{-1}$), r is the particle radius (μm), t is the time (s), ρ is the time-dependent particle radius (μm), $K(r,\rho)$ is the collision frequency function ($\mathrm{cm}^3\,\mathrm{s}^{-1}$), $D(r)$ is the molecular diffusion coefficient ($\mathrm{cm}^3\,\mathrm{s}^{-1}$), ε is the eddy diffusion coefficient due to turbulent ($\mathrm{cm}^3\,\mathrm{s}^{-1}$), $U_s(r)$ is the particle terminal settling velocity ($\mathrm{cm\,s}^{-1}$), δ is the thickness of concentration boundary layer (cm), H is the height (m), V is the volume (m^3), S is the wall surface area (m^2), Q is the volumetric ventilation rate ($\mathrm{m}^3\,\mathrm{s}^{-1}$), and $G(r,\mathrm{t}) = Q\,n_i(r,\mathrm{t})$ is the road dust generation rate (particles $\mathrm{s}^{-1}\,\mu\mathrm{m}^{-1}$) in that $n_i(r,\mathrm{t})$ is the time-dependent initial concentration of road dust of particle radius r (particles $\mathrm{cm}^{-1}\mu\mathrm{m}^{-1}$).

The left-hand side of Eq. (1) describes the change in particle concentration of road dust with size r at time t in a system volume. The first two terms on the right-hand side of Eq. (1) express the rate of formation of particles of size r due to turbulent coagulation of two particles smaller than r and the rate of loss of particle of size r due to their coagulation with particles of any other sizes including r, respectively. The third to the sixth terms describe respectively the deposition rate by turbulent diffusion, deposition rate by gravitational settling, the rate of particles removed from a system volume by ventilation airflow, and the rate of particle generation in a system volume.

Equation (1) is a nonlinear partial integro-differential equation that cannot be solved analytically. Saffman and Turner[25] has been derived an approximate expression for $K(r, \rho)$ of turbulent coagulation as,

$$K(r, \rho) = 1.30(r + \rho)^3 \left(\frac{\varepsilon_o}{\nu}\right)^{1/2}, \tag{2}$$

where ν is the kinematic viscosity ($cm^2\,s^{-1}$) and ε_o is the average energy dissipation rate ($cm^2\,s^{-1}$).

The average energy dissipation rate (ε_o) is taken to be equal to the power consumption rate per unit mass of mixing fluid and was obtained in an experiment using the standard cylindrical stirred water tank by Schwartzberg and Treybal.[26] Schwartzberg and Treybal[26] suggested that in systems where the power number is a constant, the average energy dissipation rate is proportional to $N_i^3 D^5 / T^2 H$ in which N_i is the impeller speed (rpm), D is the impeller diameter (cm), T is the tank diameter (cm), and H is the depth of liquid fills in tank (cm). For a ventilated airspace having a rectangular enclosure and volume V, the average energy dissipation rate can be redefined as,

$$\varepsilon_o = \frac{N_p N_s^3 D_s^5}{V}, \tag{3}$$

where N_p is the power number, N_s is the fan speed (rpm), and D_s is the fan diameter (cm).

The particle gravitational settling velocity ($U_s(r)$) shown in Eq. (1) can be calculated based on a high Reynolds number condition as,[27]

$$U_s(r) = \frac{2}{9} \frac{\rho_p g r^2}{\eta_a} C_{\text{slip}} \left(1 - \frac{\rho_a}{\rho_p}\right), \tag{4}$$

where ρ_a is the density of air ($g\,cm^{-3}$), ρ_p is the particle density ($g\,cm^{-3}$), g is the gravitational acceleration constant ($m\,s^{-2}$), η_a is the dynamic viscosity of air (p), and C_{slip} is the slip correlation factor,

$$C_{\text{slip}} = \left\{1 + \frac{\lambda}{2r}\left[2.541 + 0.8 \exp\left(-1.1 \frac{r}{\lambda}\right)\right]\right\}, \tag{5}$$

where λ is the mean free path of air (cm).

Assuming that road dust particles have an average radius, r_a, and there is a steady-state road dust generation rate, Eq. (1) can be rewritten as,

$$\frac{dn(t)}{dt} = -5.2r_a^3\left(\frac{\varepsilon_o}{\nu}\right)^{1/2} n^2(t) - \frac{U_s(r_a)}{H}n(t) - (D(r_a)+\varepsilon)\frac{S}{\delta V}n(t) + \frac{Q}{V}(n_i - n(t)). \tag{6}$$

To generalize the solution of Eq. (4), the following dimensionless variables were chosen as,

$$n^*(t^*) = \frac{n(t)}{n_i}, \qquad t^* = \frac{t}{(V/Q)} = \frac{t}{\bar{t}}, \tag{7}$$

where $n(t)$ is the road dust concentration at time t (particles cm^{-3}), $n^*(t^*)$ is the dimensionless road dust concentration, t^* is the dimensionless time, and $\bar{t} = V/Q$ is the mean residence time of ventilation airflow (s).

We define three dimensionless system parameters of TC, TD and GS that describe respectively the relative effects of turbulent coagulation (TC), turbulent deposition (TD), and gravitational settling (GS) as:

$$\mathrm{TC} = 5.2r_a^3\left(\frac{\varepsilon_o}{\nu}\right)^{1/2}\frac{V}{Q}n_i, \tag{8}$$

$$\mathrm{TD} = (D(r_a)+\varepsilon)\frac{S}{\delta Q}, \tag{9}$$

$$\mathrm{GS} = U_s(r_a)\frac{V}{\mathrm{HQ}}. \tag{10}$$

The terms in Eq. (6) were divided by $G(r,\mathrm{t})/V$ to obtain a ratio of road dust removed by the three mechanisms to the road dust production.

The road dust dynamics in a complete-mixing ventilated airspace can be expressed by a first-order dimensionless ordinary differential equation by substituting Eqs. (7)–(10) into Eq. (6) as,

$$\frac{dn^*(t^*)}{dt^*} = -\mathrm{TC}n^{*2}(t^*) - \mathrm{TD}n^*(t^*) - \mathrm{GS}n^*(t^*) - n^*(t^*) + 1. \tag{11}$$

The initial condition of the system is given as,

$$n^*(t^*) = n^*(t^*=0) = n^*(0). \tag{12}$$

Equation (11) subjects to Eq. (12) can be solved analytically and numerically. The road dust concentration removed by TC, TD and GS can be obtained from Eq. (7) as,

$$n(t) = n_i(1 - n^*(\infty)), \tag{13}$$

where

$$n^*(\infty) = -\frac{(\mathrm{TD}+\mathrm{GS}+1)}{2\mathrm{TC}} + \sqrt{\frac{1}{\mathrm{TC}} + \frac{1}{4}\left(\frac{\mathrm{TD}+\mathrm{GS}+1}{\mathrm{TC}}\right)^2}. \tag{14}$$

The term $n^*(\infty)$ in Eq. (14) represents the proportion of road dust removed by ventilation.

To investigate the influence of ventilation airflow patterns on the road dust concentration, three simple model cases will be discussed in details: (i) the complete-mixing system, (ii) the displacement system, and (iii) the short-circuiting system. The ventilated airspace can be divided into two equal compartments where the lower compartment represents the occupation zone (Figure 3). Complete-mixing is assumed within each compartment, whereas the mixing between the two compartments is expressed by the recycle airflow rate or secondary airflow rate.[28]

The secondary airflow rate is assumed to be entirely induced by entrainment air into the jet stream from the supplied air duct. ASHRAE[28] suggests that the entrainment ratio (β) can be used to characterize the properties of the secondary airflow rate. The actual values of the entrainment ratio depend to some extent on the relative position between the supply and exhaust position, and size, shape of the nozzle or air jet. ASHRAE[28] gives a simple entrainment concept in estimating the entrainment ratio as: $\beta = \left((2/K')(X/H_0)\right)^{1/2}$, where K' is the proportionality constant, approximate value of 7; X is the distance from face of outlet (m); and H_0 is the width of air inlet (m).

Equation (11) is the governing equation for complete-mixing ventilation system shown in Figure 3A. In displacement system (Fig. 3B), the supply and exhaust air locations are placed far apart and the ventilation airflow is forced to pass across the enclosure. When road dust is introduced into occupation zone, the mass balance gives the following expressions for road dust concentrations in compartments 1 and 2,

$$\frac{dn_1^*(t^*)}{dt^*} = -\mathrm{TC}n_1^{*2}(t^*) - \left(\mathrm{TD}\left(\frac{w_1}{k_1}\right) + \mathrm{GS} + \frac{(1+\beta)}{k_1}\right)n_1^*(t^*) + \frac{\beta}{k_1}n_2^*(t^*), \tag{15a}$$

$$\frac{dn_2^*(t^*)}{dt^*} = -\mathrm{TC}n_2^{*2}(t^*) - \left(\mathrm{TD}\left(\frac{w_2}{k_2}\right) + \frac{\mathrm{GS}}{f} + \frac{(1+\beta)}{k_2}\right)n_2^*(t^*) + \frac{1+\beta}{k_2}n_1^*(t^*), \tag{15b}$$

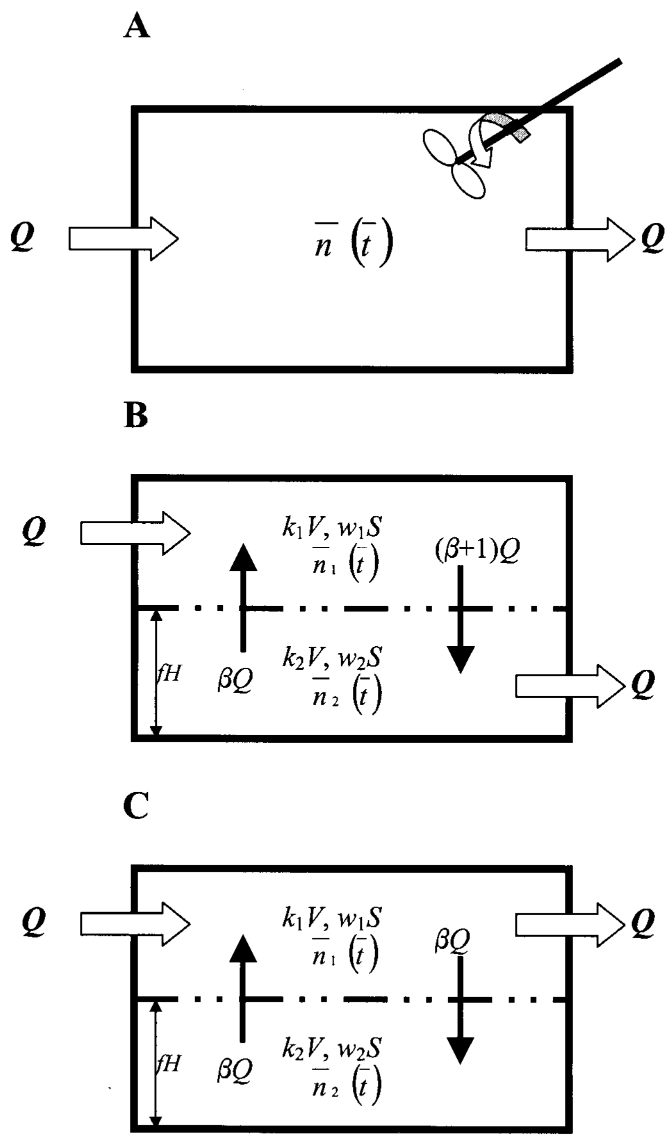

Figure 3. Inlet-exhaust configuration for ventilation systems: (A) complete-mixing, (B) displacement and (C) short-circuiting systems.

where k_i is the fractional air volume of system for compartments 1 and 2, w_i is the fractional wall surface of system for compartments 1 and 2, and f is the fractional height of system.

In the short-circuiting ventilation system (Fig. 3C) there is a risk of short-circuiting between the inlet and exhaust air location usually because of their closeness or poor mixing. In terms of the short-circuiting system, the mass balance equations become,

$$\frac{dn_1^*(t^*)}{dt^*} = -\mathrm{TC}n_1^{*2}(t^*) - \left(\mathrm{TD}\left(\frac{w_1}{k_1}\right) + \mathrm{GS} + \frac{(1+\beta)}{k_1}\right)n_1^*(t^*) + \frac{\beta}{k_1}n_2^*(t^*), \tag{16a}$$

$$\frac{dn_2^*(t^*)}{dt^*} = -\mathrm{TC}n_2^{*2}(t^*) - \left(\mathrm{TD}\left(\frac{w_2}{k_2}\right) + \frac{\mathrm{GS}}{f} + \frac{\beta}{k_2}\right)n_2^*(t^*) + \frac{\beta}{k_2}n_1^*(t^*). \tag{16b}$$

In complete-mixing and displacement systems, Eq. (11) that describes complete-mixing was modified to account for mixing between two compartments and yet maintain complete-mixing within each compartment.

RESULTS AND DISCUSSION

Particle Size Distribution

Experimental results show that the particle size distributions of road dust followed by a lognormal distribution with geometric mean diameters (gmd) (which is based on number) of 1.1 and 1.06 μm and geometric standard deviations (gsd) of 2.56 and 2.62, respectively, for urban and suburban areas. Figure 4 presents the lognormal size distribution model fitted to the experimental data for road dust obtained from urban and suburban areas.

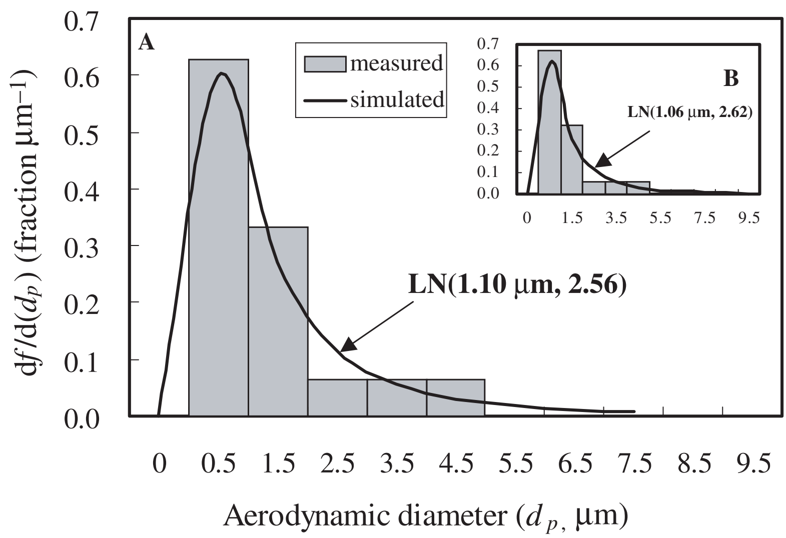

Figure 4. Lognormal size distribution model fitted to the experimental data for airborne road dust obtained from (A) urban and (B) suburban areas of the north Taiwan region.

Our data therefore demonstrate that the main contribution from road dust is $PM_{2.5}$ in north Taiwan region. To develop a better control strategy, estimation of the emission factors of $PM_{2.5}$ contribution from road dust becomes an important issue.

Dynamic Behavior Prediction and Verification

In order to investigate the effects of TC, TD, and GS on the removal dynamic behavior of airborne road dust, simulations were performed to show the significances. Initial particle distribution, particle concentration, and airflow rate was measured to calculate the experimental TC, TD, and GS values.

Figure 5 shows a dimensionless road dust particle concentration as a function of dimensionless time based on the mean residence time at different values of TC. The effect of TC on the change in total road dust particle concentration can be estimated from Figure 5 for TD = 0.123 and GS = 0.347 calculated based on the average particle diameter of 1.1 μm AED. Road dust particle concentrations increase gradually with time and then attain equilibrium. When both effects of coagulation and deposition are ignored, the road dust particle concentration increases to a higher equilibrium level, indicating that road dust is removed by ventilation only (i.e., TC = TD = GS = 0). Figure 5 also shows that the steady-state road dust concentration decreases with an increase in turbulent coagulation.

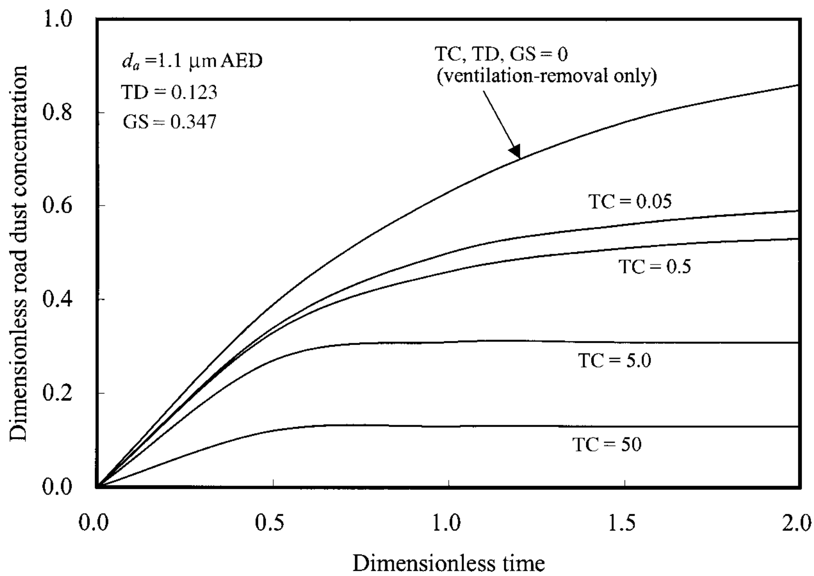

Figure 5. Increase in airborne road dust concentration with time for different values of TC based on an average particle diameter of 1.1 μm AED.

A comparison of model predictions with the observations of the removal dynamics of airborne road dust subject to different ventilation modes, ventilation rates and generation rates in an environment chamber is shown in Figures 6 and 7. Figures 6 and 7 show the time-dependent changes in particle concentration of road dust together with corresponding theoretical curves calculated via Eqs. (15) and (16) for displacement and short-circuiting ventilation systems, respectively. Table 1 gives the input parameters used in the model simulations.

The average particle diameter of road dust was 1.1 μm AED. In comparing experimental data with those calculated, the value of the concentration boundary layer thickness (δ) used in the calculation of TD was selected to be 0.085 cm, which was obtained experimentally in the study by Van de Vate.[30] Figures 6 and 7 show that the experimental particle concentrations increase gradually with time and reach steady-state according to values of TC, TD, and GS. Measured particle concentrations reached steady-state faster than those predicted. During the transient phases, the particle concentrations in a displacement system approaches steady-state faster than that in a short-circuiting system (Figs. 6 and 7). If the TC, TD, and GS values were zero, the exhaust concentrations for ventilation systems would be the same.

Model performance was evaluated by the root mean squared error (RMSE), computed from

$$\mathrm{RMSE} = \sqrt{\frac{\sum_{i=1}^{N} [C_{m,i} - C_{p,i}]^2}{N}}, \tag{17}$$

where N denotes the number of measurements and $C_{m,i}$ and $C_{p,i}$ represent the measured and predicted concentrations, respectively, corresponding to data point i. Table 2 list the RMSE values for the model performances, indicating that RMSE values ranged from 1.27 to 4.09 mg m^{-3}. The measured road dust concentrations are correlated with simulated in Figure 8. Measured values match the simulated with an r^2 value of 0.93. The overall RMSE value of 2.36 ± 1.05 mg m^{-3} is low, considering that the average standard errors of the measurements are already 1.50 mg m^{-3}.

Figures 6 and 7 also indicate that the values of TC are small for the experimental data and thus the deposition mechanisms (TD and GS) dominant the behavior of road dust and agree with the predicted curve obtained when assuming a δ value of 0.085 cm when the airborne road dust is uniformly mixed within the ventilated airspace.

Overall the predicted particle concentrations of airborne road dust agreed well with the measurements, however, a higher discrepancy was observed at lower airflow rates (Table 2). The reason may be that the assumption of complete-mixing used in deriving the system equation dose not hold as well for the low airflow rate since the density difference between

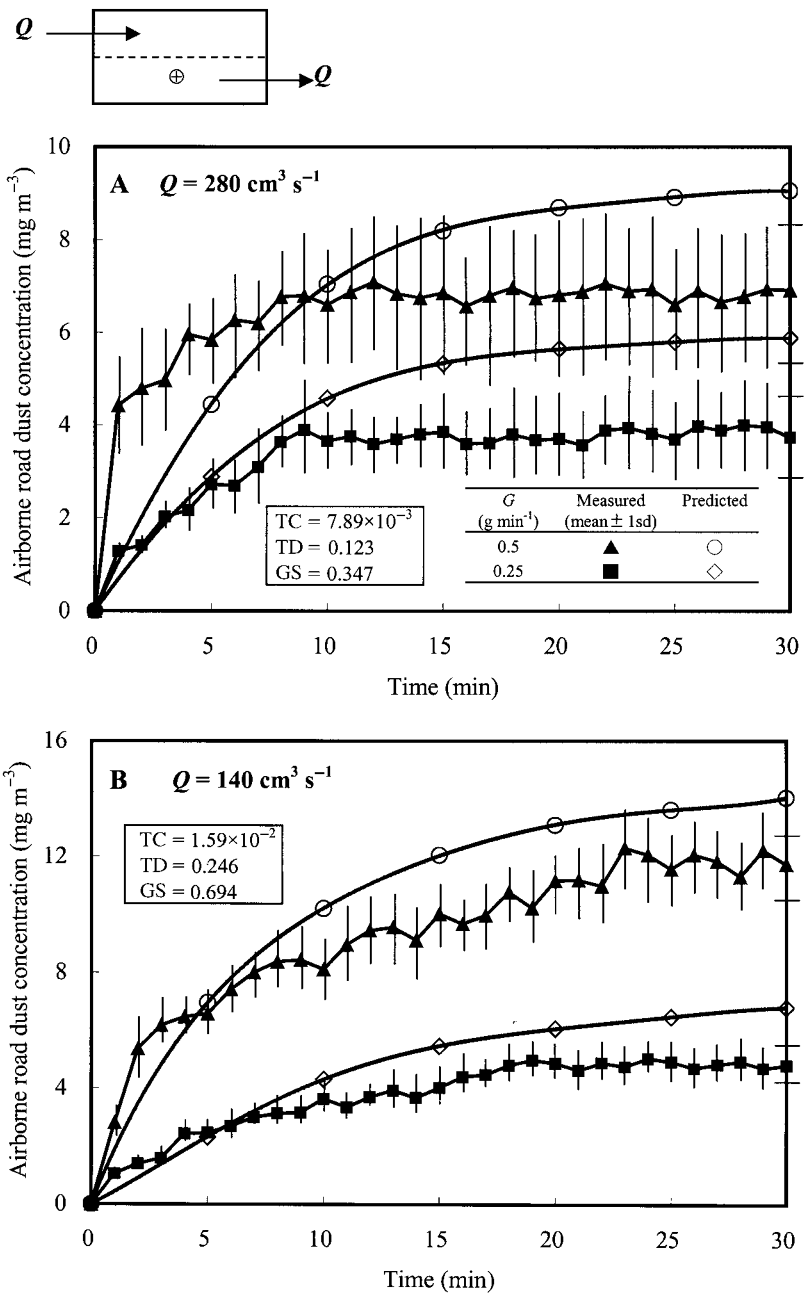

Figure 6. A comparison of model prediction with the measurements of the removal dynamics of airborne road dust in a displacement ventilation system with two generation rates of 0.5 and 0.25 g min^{-1} for (A) $Q = 280\,\text{cm}^3\,\text{s}^{-1}$ and (B) $Q = 280\,\text{cm}^3\,\text{s}^{-1}$. Error bars show one standard deviation from the mean ($n = 12$).

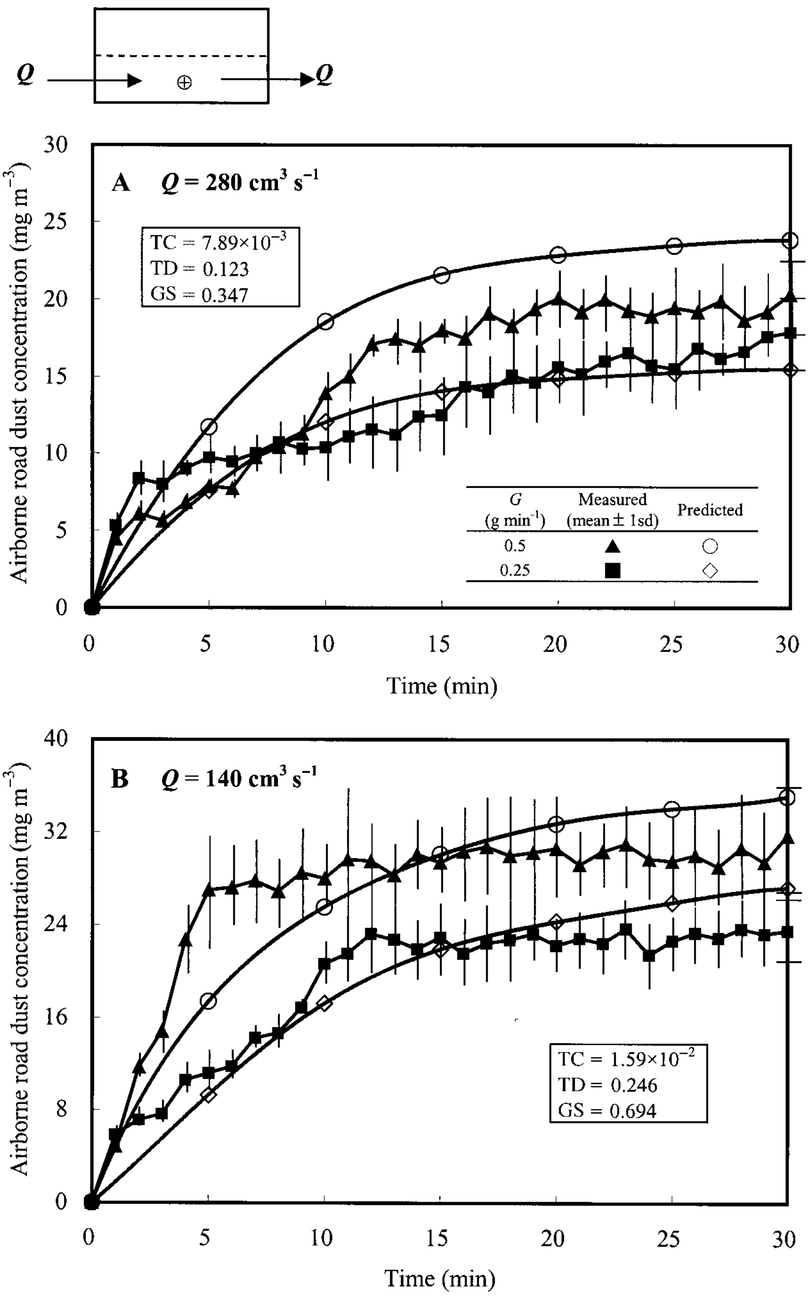

Figure 7. A comparison of model prediction with the measurements of the removal dynamics of airborne road dust in a short-circuiting ventilation system with two generation rates of 0.5 and 0.25 g min^{-1} for (A) $Q = 280\,\text{cm}^3\,\text{s}^{-1}$ and (B) $Q = 280\,\text{cm}^3\,\text{s}^{-1}$. Error bars show one standard deviation from the mean ($n = 12$).

Table 1. Input Parameters Used in the Model Simulation

Geometric parameters	
Chamber volume, $V = 7.29 \times 10^5\,cm^3$	
Chamber surface area, $S = 4.05 \times 10^4\,cm^2$	
Chamber height, $H = 90\,cm$	
$w_i = k_i = f = 0.5$	
System Parameters	
Ventilation airflow rate, $Q = 280\,cm^3\,s^{-1}$; $140\,cm^3\,s^{-1}$	
Entrainment ratio, $\beta = 2.27$[a]	
Temperature $= 27 \pm 0.5°C$	
Barometric pressure $= 1$ atm	
Average particle diameter $d_a = 1.1\,\mu m$ AED	
Kinematic viscosity of air at 27°C, $\nu = 0.158\,cm^2\,s^{-1}$[b]	
Particle settling velocity, $U_s(r) = 0.012\,cm\,s^{-1}$[c]	
Effective diffusion coefficient, $D(r) + \epsilon = 7.2 \times 10^{-5}\,cm^2\,s^{-1}$[d]	
Average energy dissipation rate, $\epsilon_0 \sim 2.5 \times 10^6\,cm^2\,s^{-3}$[e]	
Thickness of concentration boundary layer, $\delta = 0.085\,cm$[f]	
Initial road dust concentration, $n_i = 108\,cm^{-3}$; $54\,cm^{-3}$	

[a]Calculated based on the entrainment theory:[28] $\beta = ((2/K')(X/H_0))^{1/2} = ((2/7)\times\ (90/5))^{1/2} = 2.27$.
[b]Adapted from Hinds.[27]
[c]Calculated based on Eq. (4).
[d]Adapted from Davies.[29]
[e]Adapted from Okuyama and Kousaka.[23]
[f]Adapted from Van de Vate.[30]

Table 2. RMSE Values for the Model Performances

Ventilation System	Ventilation Rate Q ($cm^3\,s^{-1}$)	Road Dust Generation Rate G ($g\,min^{-1}$)	RMSE ($mg\,m^{-3}$)
Displacement	280	0.5	1.81
	280	0.25	1.49
	140	0.5	1.83
	140	0.25	1.27
Short-circuiting	280	0.5	4.04
	280	0.25	1.76
	140	0.5	4.09
	140	0.25	2.62

road dust and air and the electrostatic effect of dust particle may have been a factor. Therefore, a significant departure from homogeneity might be expected. Moreover, airborne road dust may undergo some hygroscopic growth in the high humidity environment during the chamber test. If the fine airborne road dust between 0.5 and 1 μm can grow to large sizes between 1.5 and 2.75 μm, then this increase will result in a large settling and deposition rates of airborne road dust to the surfaces.

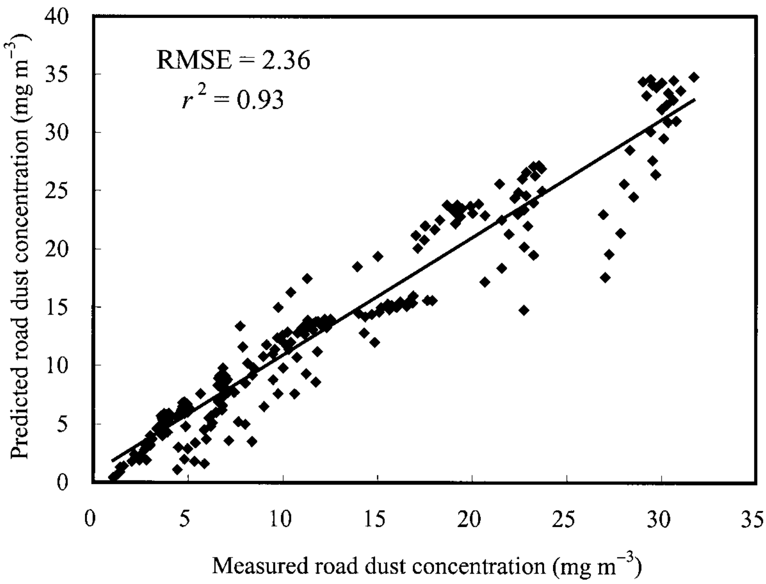

Figure 8. Measured versus predicted airborne road dust concentrations obtained using the linear dynamic equation, showing the overall root mean squared error (RMSE) of 2.36 with the coefficient of determination (r^2) of 0.93.

Further research may focus on the determination of $PM_{2.5}$ indoor/outdoor relationships and personal concentrations by using the proposed linear dynamic model for predicting indoor levels.

CONCLUSIONS

We develop a simple modeling approach represented by a linear dynamic equation in describing the removal of airborne road dust from a ventilated airspace. The dynamic equation is sufficiently to take into account the simultaneous removal effects of turbulent coagulation, turbulent diffusive deposition, gravitational sedimentation, and airflow pattern within a ventilated airspace. Three system parameters, TC, TD, and GS can be used to characterize the dynamic behavior of airborne road dust undergoing turbulent coagulation, turbulent diffusive deposition, and gravitational settling in a ventilated airspace. Our results demonstrate that different ventilation systems affect particle concentration of airborne road dust removal from the ventilated airspace. The displacement ventilation system is more effective than the short-circuiting system in removing road dust.

There is no significant variation for particle size distributions of road dust obtained from urban and suburban areas in north Taiwan region and both followed a lognormal distribution with average geometric mean diameter of

$1.08 \pm 0.02\,\mu m$ and geometric standard deviation of 2.59 ± 0.03. Experimental results agreed with the predicted results (average RMSE $= 2.36 \pm 1.05\,mg\,m^{-3}$) when the concentration boundary layer thickness was 0.085 cm and the average particle diameter for road dust was 1.1 μm AED.

The dynamic response of road dust particle concentration predicted by the proposed dynamic equation derived in this analysis compares well with those measured in the environmental chamber tests. An average radius can substitute earlier equations using the time-dependent particle radius.

REFERENCES

1. Chen, W.C.; Wang, C.S.; Wei, C.C. An Assessment of Source Contributions to Ambient Aerosols in Central Taiwan. J. Air Water Manage. Associ. **1997**, *47*, 501–509.
2. Yang, H.H.; Chiang, C.F.; Hee, W.J.; Hwang, K.P.; Wu, E.M.Y. Size Distribution and Dry Deposition of Road Dust PAHs. Environ. Int. **1999**, *25*, 585–597.
3. Chiou, S.F.; Tsai, C.J. Measurement of Emission Factor of Road Dust in a Wind Tunnel. Powder Tech. **2001**, *118*, 10–15.
4. Pope, A.; Dockery, D.W. Acute Health Effects pf PM10 Pollution on Symptomatic and Asymptomatic Children. Am. Rev. Respir. Dis. **1992**, *145*, 1123–1128.
5. Dockery, D.W.; Pope, C.A.; Xu, X. An Association Between Air Pollution and Mortality in Six US Cities. N. Engl. J. Med. **1993**, *329*, 1753–1759.
6. Schwartz, J. Particulate Air Pollution and Chronic Respiratory Disease. Environ. Res. **1993**, *62*, 7–13.
7. Seaton, A.; MacNee, W.; Donaldson, K.; Godden, D. Particulate Air Pollution and Acute Health Effects. Lancent **1995**, *345*, 176–178.
8. Ackermann-Liebrich, U.A.; Leuenberger, Ph.; Scwwartz, J.; Schindler, Ch.; Monn, Ch.; SAPALDIA Team. Lung Function and Long Term Exposure to Air Pollutants in Switzerland. Am. J. Respir. Crit. Care Med. **1997**, *155*, 122–129.
9. Miguel, A.G.; Cass, G.R.; Glovsky, M.M.; Weiss, J. Allergens in Paved Road Dust and Airborne Particles. Environ. Sci. Tech. **1999**, *33*, 4159–4168.
10. Tiittanen, P.; Timonen, K.L.; Ruuskanen, J.; Mirme, A.; Pekkanen, J. Fine Particulate Air Pollution, Resuspended Road Dust and Respiratory Health Among Symptomatic Children. Eur. Respir. J. **1999**, *13*, 266–273.
11. Hirsch, T.; Neumeister, V.; Weiland, S.K.; von Mutius, E.; Hirsch, D.; Grafe, H.; Duhme, H.; Leupold, W. Traffic Exposure and Allergic Sensitization Against Latex in Children. J. Allergy Clinic. Immun. **2000**, *106*, 573–578.
12. Sanders, T,G; Addo, J.Q.; Ariniello, A.; Heiden, W.F. Relative Effectiveness of Road Dust Suppressants. J. Transport. Eng. ASCE **1997**, *123*, 393–397.
13. Tsai, C.J.; Miaw, D.Y.; Chiou, S.F.; Lin, T.Y.; Chong, J.B.; Huang, C.H.; Wang, S.H. The Investigation of Domestic Control Technologies for Fugitive Particle Pollutants. The 1998 International Conference on Aerosol Science and Technology, Ping Tong, Taiwan, 1998; 417–426.

14. Cheng, M.T.; Lin, Y.C.; Jeang, S.J.; Yen, S.L. Characteristics and Emission Factor of Traffic Road Dust. The 1998 International Conference on Aerosol Science and Technology, Ping Tong, Taiwan, 1998; 427–435.
15. Friedlander, S.K. *Smoke, Dust and Haze. Fundamentals of Aerosol Behavior*. John Wiley & Sons: New York, 1977.
16. Okuyama, K.; Kousaka, Y.; Adachi, M. Coagulation and Deposition of Aerosol Particles in a Flow Type Chamber. J. Aerosol Sci. **1980**, *11*, 11–22.
17. Rogge, W.F.; Hildemann, L.M.; Mazurek, M.A.; Cass, G.R.; Simoneit, B.R.T. Mathematical Modeling of Atmospheric Fine Particle-Associated Primary Organic Compound Concentrations. J. Geophy. Res.-Atmos. **1996**, *101*, 19379–19394.
18. Kleeman, M.J.; Cass, G.R. Source Concentrations to the Size and Composition Distribution of Urban Particulate Air Pollution. Atmos. Environ. **1998**, *32*, 2803–2816.
19. Wang, I.T.; Chico, T.; Huang, Y.H.; Farber, R.J. Development, Evaluation, and Application of a Primary Aerosol Model. J. Air Waste Manage. Associ. **1999**, *49*, 57–68.
20. Liao, C.M.; Singh, S. Characterizing Odor Adsorption on Dust Surface Based on Age and Size Distributions of Airborne Dust in a Ventilated Airspace. J. Environ. Sci. Health **1998**, *A33*, 1091–1117.
21. Liao, C.M.; Chen, J.S.; Chen, J.W. Dynamic Model for Predicting Dust-Borne Odour Concentrations in Ventilated Animal Housing. Appl. Math. Modelling **2000**, *24*, 131–145.
22. Greenfield, M.A.; Koontz, R.L.; Hausknecht, D.F. Comparison of Experiment and Theory for the Coagulation of Aerosols. J. Colloid. Int. Sci. **1971**, *35*, 102–113.
23. Okuyama, K.; Kousaka, Y. Turbulent Coagulation of Aerosols in a Stirred Tank. J. Chem. Eng. Japan **1977**, *10*, 142–147.
24. Liao, C.M.; Chen, J.W.; Chen, J.S.; Liang, H.M. A Transfer Function Model to Describe Odor Causing VOcs Transport in a Ventilated Airspace with Mixing/Adsorption Heterogeneity. Appl. Math. Modelling **2001**, *25*, 1071–1087.
25. Saffman, P.G.; Turner, J.S. On the Collision of Drops in Turbulent Clouds. J. Fluid Mech. **1956**, *1*, 16–30.
26. Schwartzberg, H.G.; Treybal, R.E. Fluid and Particle Motion in Turbulent Stirred Tank. Ind. Eng. Chem. Fundam. **1968**, *7*, 1–6.
27. Hinds, W.C. Aerosol Technology. *Properties, Behavior, and Measurement of Airborne Particles*. 2nd Ed.; John Wiley & Sons: New York, 1999.
28. ASHRAE. *ASHRAE Handbook of Fundamentals*. American Society of Heating, Refrigeration, and Air Conditioning Engineers: New York, 1993.
29. Davies, C.N. Deposition from Moving Aerosols. In *Aerosol Science*, Davies, C.N., Ed.; Academic Press: New York, 1966; 393–446.
30. Van de Vate, J.F. The Thickness of the Stagnant Air Layer in Aerosol Contaminants and the Aerodynamic Diameter of Aggregates of Small Spheres. J. Collid. Int. Sci. **1972**, *41*, 104–107.

Received November 27, 2001